

## Statistical Distribution of Wind at the Kagoshima Space Center

By

Yasunori MATOGAWA

*Summary:* Wind data from the balloon tracking radar at KSC (the Kagoshima Space Center, University of Tokyo) are utilized to determine statistical wind distributions. The analysis is based on the bivariate normal distribution method. Some of the results obtained by the binormal analysis are compared with those obtained empirically. The assumption of a circular distribution is shown to be invalid for winds at KSC.

### 1. INTRODUCTION

A knowledge of winds and their distribution is indispensable to establish structural design and dispersion criteria of rocket vehicles. In the past most treatments of wind data have been restricted to particularly the cumulative percentage frequency method [1]. Results from these studies are usually limited in both scope and accuracy. Statistical approach to the estimation of wind distributions is therefore desirable which is not adversely affected by extreme values in the wind data. The method employed in this report is believed to satisfy this requirement.

Winds are three dimensional but for most purposes they are considered only in their two dimensional form on horizontal planes. Although exceptions are noted, winds in the free atmosphere in the horizontal surfaces may be considered to be normally distributed in the general bivariate sense. Crutcher [2] suggested this binormal distribution method and discussed briefly its implementation. Weaver and others [3] made use of this binormal method to determine parameters describing wind distributions at NASA Wallops Station by utilizing data from several stations. But in all these preceding studies population parameters describing probability ellipses are set to be equal to sampling statistics without notice.

Analysis methods employed in this report are based on the assumption that the orthogonal components of wind vectors are normally distributed random variables. Wind data from the balloon tracking radar at KSC are utilized to determine an elliptical wind distribution using the binormal method. Wind speed profiles obtained by this method are compared with corresponding profiles obtained by assuming the distribution to be circular and with profiles obtained by the empirical cumulative percentage frequency method.

## 2. COMPUTATIONAL PROCEDURES

## 2.1 Wind Vectors

When the population sample of wind is sufficiently large, we can assure the validity of a large sample estimate of statistical parameters of wind distribution. It is convenient to consider the zonal and meridional components of a group of wind data observed at some particular altitude as statistical samples. Geometric description of wind distribution parameters is given in Fig. 1. The following estimates can then be readily obtained as appropriate parameters for describing population characteristics of winds. These parameters are best unbiased estimates of their population parameters when population is assumed to be normally distributed.

For mean zonal wind  $\mu_u$ :

$$\bar{u} = \frac{1}{N} \sum_{i=1}^N u_i = \frac{1}{N} \sum_{i=1}^N |V_i| \sin \theta_i. \quad (1)$$

For mean meridional wind  $\mu_v$ :

$$\bar{v} = \frac{1}{N} \sum_{i=1}^N v_i = \frac{1}{N} \sum_{i=1}^N |V_i| \cos \theta_i. \quad (2)$$

For variance of zonal wind  $\sigma_u^2$ :

$$s_u^2 = \frac{1}{N-1} \sum_{i=1}^N (u_i - \bar{u})^2. \quad (3)$$

For variance of meridional wind  $\sigma_v^2$ :

$$s_v^2 = \frac{1}{N-1} \sum_{i=1}^N (v_i - \bar{v})^2. \quad (4)$$

For standard deviation of zonal wind  $\sigma_u$ :

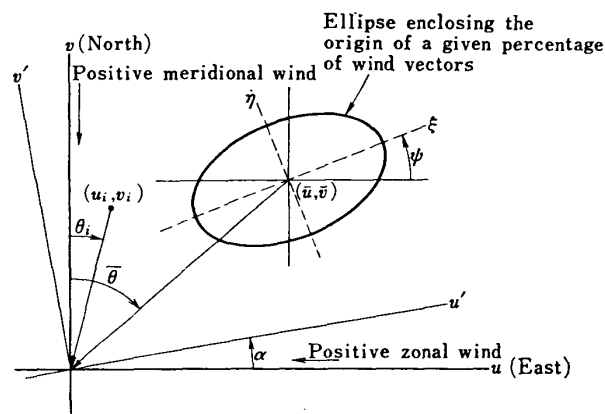


FIG. 1. Geometric description of wind distribution parameters.

$$\frac{s_u}{C_2^*} = \frac{s_u}{\frac{\sqrt{2}}{\sqrt{N-1}} \cdot \frac{\Gamma(N/2)}{\Gamma((N-1)/2)}} = \frac{s_u}{1 - \frac{1}{4N}} \quad (5)$$

For standard deviation of meridional wind  $\sigma_v$  :

$$\frac{s_v}{C_2^*} = \frac{s_v}{\frac{\sqrt{2}}{\sqrt{N-1}} \cdot \frac{\Gamma(N/2)}{\Gamma((N-1)/2)}} = \frac{s_v}{1 - \frac{1}{4N}} \quad (6)$$

For correlation coefficient  $\rho$  :

$$r = \frac{s_{uv}}{s_u s_v} = \frac{\sum_{i=1}^N (u_i - \bar{u})(v_i - \bar{v})}{\sqrt{\sum_{i=1}^N (u_i - \bar{u})^2} \sqrt{\sum_{i=1}^N (v_i - \bar{v})^2}} \quad (7)$$

These parameters have a valid meaning regardless of the sample distribution. But if a distribution of wind vectors is assumed, the foregoing parameters can be used to determine statistical estimates of wind vectors to give various useful informations as shown in the following sections.

### 2.2 Fitting of Normal Bivariate Distribution

If the vector wind components  $u$  and  $v$  are independent and are normally distributed, then, the zonal and meridional wind components are each distributed according to the univariate Gaussian distribution and the probability density functions are given as follows:

$$f(u) = \frac{1}{\sqrt{2\pi}\sigma_u} \exp \left[ -\frac{1}{2} \left( \frac{u - \mu_u}{\sigma_u} \right)^2 \right] \quad (8)$$

$$f(v) = \frac{1}{\sqrt{2\pi}\sigma_v} \exp \left[ -\frac{1}{2} \left( \frac{v - \mu_v}{\sigma_v} \right)^2 \right] \quad (9)$$

Then the wind components will have the following joint probability density which is the bivariate normal density function:

$$f(u, v) = f(u)f(v) = \frac{1}{2\pi\sigma_u\sigma_v} \exp \left[ -\frac{1}{2} \left\{ \left( \frac{u - \mu_u}{\sigma_u} \right)^2 + \left( \frac{v - \mu_v}{\sigma_v} \right)^2 \right\} \right] \quad (10)$$

Under these conditions the probability that a wind vector, terminating at the origin of the coordinate axes, will originate in a region  $S$  of the  $uv$  plane is given by

$$P(u, v) = \frac{1}{2\pi\sigma_u\sigma_v} \iint_S \exp \left[ -\frac{1}{2} \left\{ \left( \frac{u - \mu_u}{\sigma_u} \right)^2 + \left( \frac{v - \mu_v}{\sigma_v} \right)^2 \right\} \right] dudv \quad (11)$$

If the component winds are not distributed independently, then equation (11) must be modified to describe the probability:

$$P(u, v) = \frac{1}{2\pi\sigma_u\sigma_v\sqrt{1-\rho^2}} \iint_S \exp\left(-\frac{G}{2}\right) dudv \quad (12)$$

where

$$G = \frac{1}{1-\rho^2} \left[ \left( \frac{u-\mu_u}{\sigma_u} \right)^2 - \frac{2\rho(u-\mu_u)(v-\mu_v)}{\sigma_u\sigma_v} + \left( \frac{v-\mu_v}{\sigma_v} \right)^2 \right]. \quad (13)$$

The quantity  $\rho$  is the correlation coefficient and describes the degree of interdependence between  $u$  and  $v$  as follows:

$$\rho = \frac{\sigma_{uv}}{\sigma_u\sigma_v}. \quad (14)$$

### 2.3 Probability Ellipses

For constant values of  $G$ , equation (13) defines a family of homothetic ellipses (common origin, common axes, and constant eccentricity) in the  $uv$  plane. Therefore, the probability distributions expressed by equation (12) are referred to as elliptical binormal distribution. If the origin of the  $u, v$  axes is translated to a point  $(\mu_u, \mu_v)$  and then rotated through the angle

$$\phi = \frac{1}{2} \tan^{-1} \frac{2\rho\sigma_u\sigma_v}{\sigma_u^2 - \sigma_v^2} \quad (15)$$

it can be shown that in this new coordinate system  $O' - \xi\eta$  (Fig. 1) the probability density and the probability can be written as follows:

$$f(u, v) = f(\xi, \eta) = \frac{1}{2\pi\sigma_\xi\sigma_\eta} \exp \left[ -\frac{1}{2} \left\{ \left( \frac{\xi}{\sigma_\xi} \right)^2 + \left( \frac{\eta}{\sigma_\eta} \right)^2 \right\} \right] \quad (16)$$

$$P(u, v) = P(\xi, \eta) = \frac{1}{2\pi\sigma_\xi\sigma_\eta} \iint_S \exp \left[ -\frac{1}{2} \left\{ \left( \frac{\xi}{\sigma_\xi} \right)^2 + \left( \frac{\eta}{\sigma_\eta} \right)^2 \right\} \right] d\xi d\eta. \quad (17)$$

This translation and rotation defines a new set of axes for which  $\rho=0$ .

Since equations (12) and (17) are equal over the same region of integration, it can be shown that

$$\sigma_\xi\sigma_\eta = \sigma_u\sigma_v\sqrt{1-\rho^2} \quad (18)$$

and

$$\sigma_\xi^2 + \sigma_\eta^2 = \sigma_u^2 + \sigma_v^2. \quad (19)$$

If  $G=C^2=\text{constant}$ , equation (13) can be written as

$$\frac{\xi^2}{\sigma_\xi^2} + \frac{\eta^2}{\sigma_\eta^2} = G = C^2 \quad (20)$$

and the semiaxes of any one of these ellipses become  $C\sigma_\xi$  and  $C\sigma_\eta$ . Illustrated in

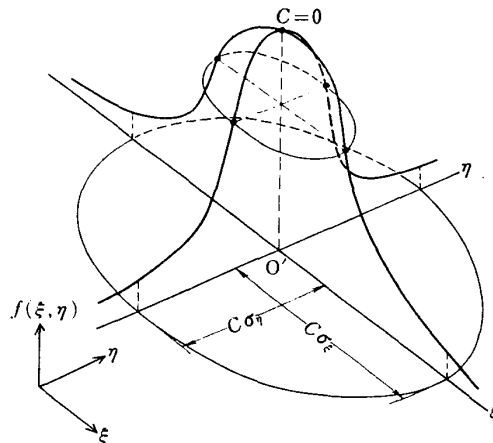


FIG. 2. Feature of probability density function.

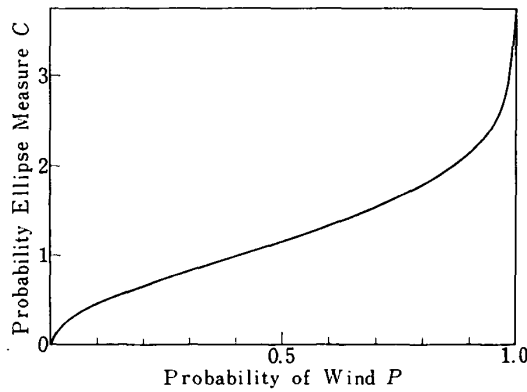


FIG. 3. Probability ellipse measure.

Fig. 2 is the feature of probability density function  $f(\xi, \eta)$  expressed in equation (16). From this figure can be observed the fact the semiaxes become larger as the measure  $C$  gets larger. As the differential area of an ellipse given by equation (20) is  $2\pi C\sigma_\xi\sigma_\eta dC$ , equation (17) can be written as

$$P(\xi, \eta) = \int_0^C \exp\left(-\frac{C^2}{2}\right) C dC = 1 - \exp\left(-\frac{C^2}{2}\right). \quad (21)$$

The relation expressed in equation (21) is illustrated in Fig. 3. Equation (21) gives the probability that a wind vector will originate inside an ellipse given by equation (20) and will terminate at the origin  $u=v=0$ . Thus, for any probability  $P$ , semiaxes of the probability ellipse are given by the following equations:

$$a = \sqrt{2 \log\left(\frac{1}{1-P}\right)} \sigma_\xi \quad (22)$$

$$b = \sqrt{2 \log\left(\frac{1}{1-P}\right)} \sigma_\eta \quad (23)$$

Hence, if a normally distributed set of wind vectors is observed, it will be found that the vectors originating from a point on or within an ellipse centered at  $(\mu_u, \mu_v)$

with semimajor and semiminor axes given by  $C\sigma_\xi$  and  $C\sigma_\eta$ , will have a probability  $P$  of occurrence, where  $C$  and  $P$  are related as shown in equation (21). The major axis of this ellipse will be rotated through an angle  $\phi$  with respect to the  $u$  (zonal) axis. Obviously, if  $\sigma_u = \sigma_v = \sigma$  and if  $\rho = 0$ , then the ellipse becomes a circle. In this case the relations defined by equations (12) and (13) are referred to as circular binormal distribution.

#### 2.4 Wind-Speed and Wind-Direction Probability Profiles

Wind-speed and wind-direction probabilities are found by integration of equation (12) over appropriate regions. The integration is simpler if the following substitutions are made:

$$\begin{aligned} u &= V \sin \theta & \bar{u} &= \tilde{V} \sin \tilde{\theta} \\ v &= V \cos \theta & \bar{v} &= \tilde{V} \cos \tilde{\theta} \\ R &= \frac{V}{\sigma_u} & \tilde{R} &= \frac{\tilde{V}}{\sigma_u} \\ c &= \frac{\sigma_v}{\sigma_u}. \end{aligned} \quad (24)$$

Then equation (12) becomes

$$P(R_1 \leq R \leq R_2, \theta_1 \leq \theta \leq \theta_2) = A \int_{\theta_1}^{\theta_2} \int_{R_1}^{R_2} \exp \left[ -\frac{B}{2(1-\rho^2)} \right] R dR d\theta \quad (25)$$

where

$$A = \frac{1}{2\pi c \sqrt{1-\rho^2}} \exp \left[ -\frac{\tilde{R}^2}{2(1-\rho^2)} \left( \sin^2 \tilde{\theta} - \frac{2\rho \sin \tilde{\theta} \cos \tilde{\theta}}{c} + \frac{\cos^2 \tilde{\theta}}{c^2} \right) \right] \quad (26)$$

and

$$\begin{aligned} B &= R^2 \left( \sin^2 \theta - \frac{2\rho \sin \theta \cos \theta}{c} + \frac{\cos^2 \theta}{c^2} \right) \\ &\quad - 2R \tilde{R} \left\{ \sin \theta \sin \tilde{\theta} - \frac{\rho}{c} \sin (\theta + \tilde{\theta}) + \frac{\cos \theta \cos \tilde{\theta}}{c^2} \right\}. \end{aligned} \quad (27)$$

For the special case of the circular distribution, equation (25) reduces to

$$\begin{aligned} P(R_1 \leq R \leq R_2, \phi_1 \leq \phi \leq \phi_2) \\ = \frac{1}{2\pi} \exp \left( -\frac{\tilde{R}^2}{2} \right) \int_{\phi_1}^{\phi_2} \int_{R_1}^{R_2} \exp \left[ -\frac{R^2 - 2R\tilde{R} \cos \phi}{2} \right] R dR d\phi \end{aligned} \quad (28)$$

where

$$\sigma_u = \sigma_v = \sigma \quad \text{and} \quad \phi = \theta - \tilde{\theta}.$$

If equation (25) or equation (28) is integrated over a region described by a circle around the origin of the  $u, v$  coordinate axes (with the origin of the distribution at

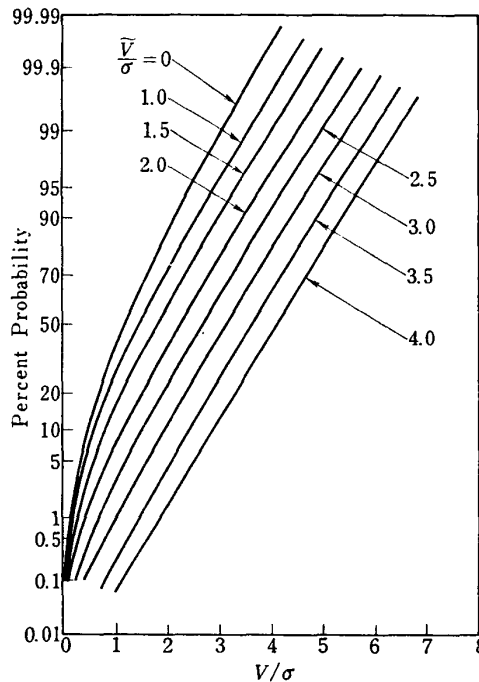


FIG. 4. Wind speed probability curves for circular bivariate normal distributions.

$\bar{u}, \bar{v}$ ), then the resulting probability will be that of a wind vector originating on or within this circle and terminating at  $u=v=0$ . The integration limits of equation (25) are then  $\theta_1=0$  and  $\theta_2=2\pi$  and  $R_1=0$  and  $R_2=R_2$ . Since the probability is a function of the variable  $R_2$ , this integral is solved by substituting the desired value of probability into the left-hand side and a value of  $R_2$  which satisfies equation (25) is found by iteration. For equation (28) a similar procedure is followed with  $\phi_1=0$  and  $\phi_2=2\pi$  and  $R_1=0$  and  $R_2=R_2$ . For the elliptical distribution (equation 25), the probability is a function of  $(V/\sigma_u, \tilde{V}/\sigma_u, \tilde{\theta}, c, \rho)$  and, therefore, it is not practical to generate a table or set of curves giving general solutions. However, for the circular distribution (equation 28), a simple table can be constructed for  $P$  as a function of  $\tilde{V}/\sigma$  and  $V/\sigma$ ; a plot of such a table is presented in Fig. 4.

In order to find the probability that a wind (including all wind speeds) will blow from a region bounded by  $\theta=0$  and  $\theta=\theta_2$  (or  $\phi=0$  and  $\phi=\phi_2$ ), the limits of integration of equation (25) are changed to  $\theta_1=0$  and  $\theta_2=\theta_2$  and  $R_1=0$  and  $R_2 \rightarrow \infty$  and of equation (28) to  $\phi_1=0$  and  $\phi_2=\phi_2$  and  $R_1=0$  and  $R_2 \rightarrow \infty$ . In performing the numerical integration, the upper limit of  $R$  was, of course, limited to a finite but high value. The elliptical binormal distribution again requires an extensive general table, and a particular solution for a given set of variables is all that is generally practical. The circular distribution once more reduces to a sufficiently small set of variables with  $P$  depending on  $\phi$  and  $\tilde{V}/\sigma$ , a general solution can be given as was presented in Fig. 5. The probability of a wind blowing from a region bounded by radius vectors having angles of  $\theta_1$  and  $\theta_2$  (or  $\phi_1$  and  $\phi_2$ ) is

$$P(\theta_2) - P(\theta_1) \quad (\theta_2 > \theta_1)$$

and

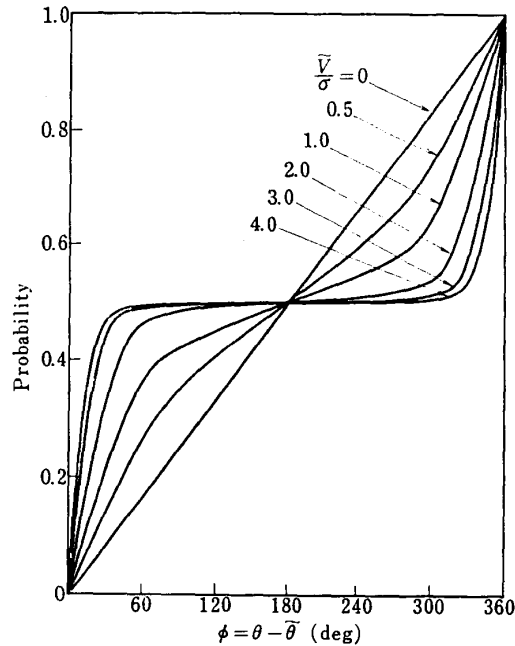


FIG. 5. Wind direction probability curves for circular bivariate normal distributions.

$$1 + [P(\theta_2) - P(\theta_1)] \quad (\theta_1 > \theta_2).$$

Obviously, the probability of a wind of a given magnitude coming from a specified range of direction can also be found by using equations (25) and (28).

### 2.5 Component Wind Probability Envelopes

The projection of the wind distribution function on an axis gives the marginal distribution of the wind vectors along that axis; for example, the marginal distribution of  $u$  defines the probability of occurrence of the east-west component of wind having the value  $u$  regardless of the value of  $v$ . In practice, one is usually interested in the marginal distributions of a set of orthogonal components, such as down-range and cross-range components. The marginal density or frequency functions for  $u$  and  $v$  are

$$f(u) = \frac{1}{\sqrt{2\pi}\sigma_u} \exp \left[ -\frac{1}{2} \left( \frac{u - \mu_u}{\sigma_u} \right)^2 \right] \quad (29)$$

$$f(v) = \frac{1}{\sqrt{2\pi}\sigma_v} \exp \left[ -\frac{1}{2} \left( \frac{v - \mu_v}{\sigma_v} \right)^2 \right]. \quad (30)$$

Equations (29) and (30) are identical with equations (8) and (9); that is, the marginal distributions are merely the univariate normal distributions along the axes of interest. The integral of this function is given in any standard mathematical table. Therefore, probability envelopes expressed in standard deviations from the mean wind speed can be determined very simply; for example, 99.73 percent of all east-west winds will be within a value of plus or minus three standard deviations of the mean east-west wind.

For a set of axes  $u'$  and  $v'$  rotated through an angle  $\alpha$  from the  $u, v$  axes, the wind component probability envelopes are defined by addition of multiples of the standard deviations along these  $(u', v')$  axes to the value of the mean wind along these axes. Rotating the axes gives

$$u' = u \cos \alpha + v \sin \alpha \quad (31)$$

$$v' = -u \sin \alpha + v \cos \alpha \quad (32)$$

and

$$\bar{u}' = \bar{u} \cos \alpha + \bar{v} \sin \alpha \quad (33)$$

$$\bar{v}' = -\bar{u} \sin \alpha + \bar{v} \cos \alpha \quad (34)$$

Since

$$s_u = \sqrt{\frac{1}{N-1} \sum_{i=1}^N (u_i - \bar{u})^2} \quad (35)$$

then,

$$s_{u'} = \sqrt{\frac{1}{N-1} \sum_{i=1}^N [(u_i - \bar{u}) \cos \alpha + (v_i - \bar{v}) \sin \alpha]^2} \quad (36)$$

which reduces to

$$s_{u'} = \sqrt{s_u^2 \cos^2 \alpha + s_v^2 \sin^2 \alpha + 2\rho s_u s_v \sin \alpha \cos \alpha} \quad (37)$$

Similarly,

$$s_{v'} = \sqrt{s_u^2 \sin^2 \alpha + s_v^2 \cos^2 \alpha - 2\rho s_u s_v \sin \alpha \cos \alpha} \quad (38)$$

For the circular distribution, the mean values are the same as those given by equations (33) and (34) and the unbiased estimate of the standard deviation is simply  $s$ . If a distribution has a small eccentricity, a circular distribution standard deviation may be approximated by

$$s = \sqrt{\frac{s_u^2 + s_v^2}{2}} \quad (39)$$

### 3. RESULTS AND DISCUSSION

#### 3.1 Data Source

Wind data in Table 1 were used as a basis for determining the KSC wind distributions. The data were obtained by use of balloon tracking radar at KSC. Systems of the radar are described in reference [4].

#### 3.2 Statistical Parameters

With the use of basic parameters obtained from equations (1) to (7), various quantities defining the wind distribution at KSC are presented in Table 2.

TABLE 1. Number of wind observations at KSC  
(1967~1974)

Altitude (m)	Number of observations	
	Winter	Summer
25	233	266
75	233	266
125	233	266
175	233	266
225	233	266
275	233	266
350	233	266
450	233	266
575	233	266
750	233	266
1000	233	266
1375	211	252
2000	207	251
3150	203	245
5600	174	193
11050	67	116

### 3.3 Probability Wind-Speed Profiles

One of the parameters of interest in wind-distribution probability studies is the variation with altitude of wind speeds that will not be exceeded a given percentage of the time regardless of the direction from which the wind blows. Such profiles are obtained for KSC by using the three methods discussed in the previous section: the elliptical and circular binormal theoretical distribution methods and the empirical cumulative frequency method.

Comparisons of profiles obtained by these methods are shown in Fig. 6.

The 50, 80 and 99% probability profiles determined by the elliptical method and the empirical method are in fair agreement for both winter and summer. But the circular distribution profiles are not in good agreement with those determined by considering the distribution to be elliptical.

When class intervals are used to obtain wind-speed profiles, as is done in the empirical method, the error in determining probability increases with increasing class-interval size. In the probability regions which correspond to high wind speeds, the limited number of winds sampled can influence the empirical profiles considerably; whereas, theoretical profiles are much less affected by extreme values or by bias in the data. Therefore, it is believed that the wind profiles obtained by assuming the winds to follow an elliptical binormal distribution offer the best estimates of the true probabilities for KSC, particularly for high probability profiles.

It should be noted, however, that, because of the accuracy limitations of the

TABLE 2 (a). Statistical parameters for wind distributions at KSC—winter.

Altitude m	$\bar{u}$ m/sec	$\bar{v}$ m/sec	$s_u$ m/sec	$s_v$ m/sec	$s_\xi$ m/sec	$s_\eta$ m/sec	$r$	$\phi$ deg	$\bar{V}$ m/sec	$\bar{\theta}$ deg	$s_V$ m/sec	$s$ m/sec	$\bar{V}/s$
25	- 0.972	1.076	2.454	2.054	2.645	1.801	- 0.326	- 30.64	1.450	137.91	3.200	2.263	0.641
75	- 1.714	1.693	3.393	2.871	3.826	2.262	- 0.459	- 34.95	2.409	134.65	4.445	3.143	0.767
125	- 1.865	1.880	3.801	3.516	4.363	2.788	- 0.414	- 39.66	2.648	135.23	5.178	3.661	0.723
175	- 2.122	2.030	4.080	3.991	4.773	3.131	- 0.398	- 43.41	2.937	133.73	5.707	4.036	0.728
225	- 2.449	2.014	4.292	4.271	5.099	3.264	- 0.419	- 44.67	3.171	129.43	6.055	4.282	0.741
275	- 2.713	1.985	4.631	4.196	5.156	3.532	- 0.349	- 37.12	3.362	126.19	6.249	4.419	0.761
350	- 3.016	1.968	4.765	4.193	5.188	3.656	- 0.314	- 33.89	3.601	123.13	6.347	4.488	0.802
450	- 3.527	2.011	5.093	4.235	5.390	3.850	- 0.273	- 27.88	4.060	119.69	6.624	4.684	0.867
575	- 3.938	2.059	5.481	4.627	5.931	4.034	- 0.332	- 31.41	4.444	117.60	7.173	5.072	0.876
750	- 4.716	2.041	5.772	4.822	6.266	4.160	- 0.350	- 31.35	5.139	113.40	7.521	5.318	0.966
1000	- 5.983	2.151	5.950	5.072	6.451	4.417	- 0.329	- 32.02	6.358	109.77	7.818	5.528	1.150
1375	- 7.736	2.270	6.198	4.956	6.232	4.913	- 0.080	- 9.80	8.062	106.35	7.936	5.611	1.437
2000	-10.901	1.920	6.557	5.437	6.747	5.199	0.178	21.73	11.069	99.99	8.518	6.023	1.838
3150	-15.949	0.995	6.536	6.245	7.274	5.368	0.292	40.57	15.980	93.57	9.040	6.392	2.500
5600	-20.984	2.892	11.472	11.499	14.185	7.913	0.525	44.87	21.182	97.85	16.243	11.486	1.844
11050	-51.148	- 2.242	26.302	12.642	26.472	12.281	- 0.210	- 7.35	51.197	- 92.51	29.182	20.635	2.481

TABLE 2 (b). Statistical parameters for wind distributions at KSC—summer.

Altitude m	$\bar{u}$ m/sec	$\bar{v}$ m/sec	$s_u$ m/sec	$s_v$ m/sec	$s_\xi$ m/sec	$s_\eta$ m/sec	$r$	$\phi$ deg	$\bar{V}$ m/sec	$\bar{\theta}$ deg	$s_v$ m/sec	$s$ m/sec	$\bar{V}/s$
25	0.972	—	2.552	2.113	2.602	2.059	0.137	17.93	0.976	—	3.313	2.343	0.417
75	0.972	—	3.045	2.686	3.215	2.480	0.223	30.31	0.986	—	4.060	2.871	0.343
125	0.941	—	3.392	3.207	3.694	2.854	0.246	38.58	0.980	—	4.668	3.301	0.297
175	0.888	—	3.718	3.530	3.964	3.251	0.189	37.35	0.941	—	5.127	3.625	0.260
225	0.851	—	3.958	3.772	4.219	3.477	0.185	37.71	0.946	—	5.468	3.866	0.245
275	0.857	—	4.148	3.834	4.322	3.636	0.152	31.33	0.911	—	5.648	3.994	0.228
350	0.751	—	4.406	3.784	4.477	3.699	0.114	18.41	0.796	—	5.808	4.107	0.194
450	0.520	—	4.706	3.866	4.744	3.817	0.091	12.31	0.559	—	6.090	4.307	0.130
575	0.293	—	5.083	4.053	5.085	4.050	0.023	2.82	0.510	—	6.501	4.597	0.111
750	—	—	5.299	4.172	5.313	4.155	—	6.68	0.525	—	6.744	4.769	0.110
1000	—	—	6.028	4.495	6.218	4.253	—	19.05	1.014	—	7.519	5.317	0.191
1375	—	—	6.060	4.755	6.375	4.323	—	25.01	1.871	—	7.703	5.447	0.344
2000	—	—	6.260	4.834	6.562	4.414	—	23.93	2.808	—	7.909	5.593	0.502
3150	—	—	6.173	4.858	6.349	4.626	—	19.96	4.014	—	7.855	5.555	0.723
5600	—	—	7.173	4.924	7.208	4.874	0.104	7.59	4.910	—	8.700	6.152	0.798
11050	—	—	9.523	8.919	9.824	8.588	—	30.35	5.594	—	13.047	9.226	0.606

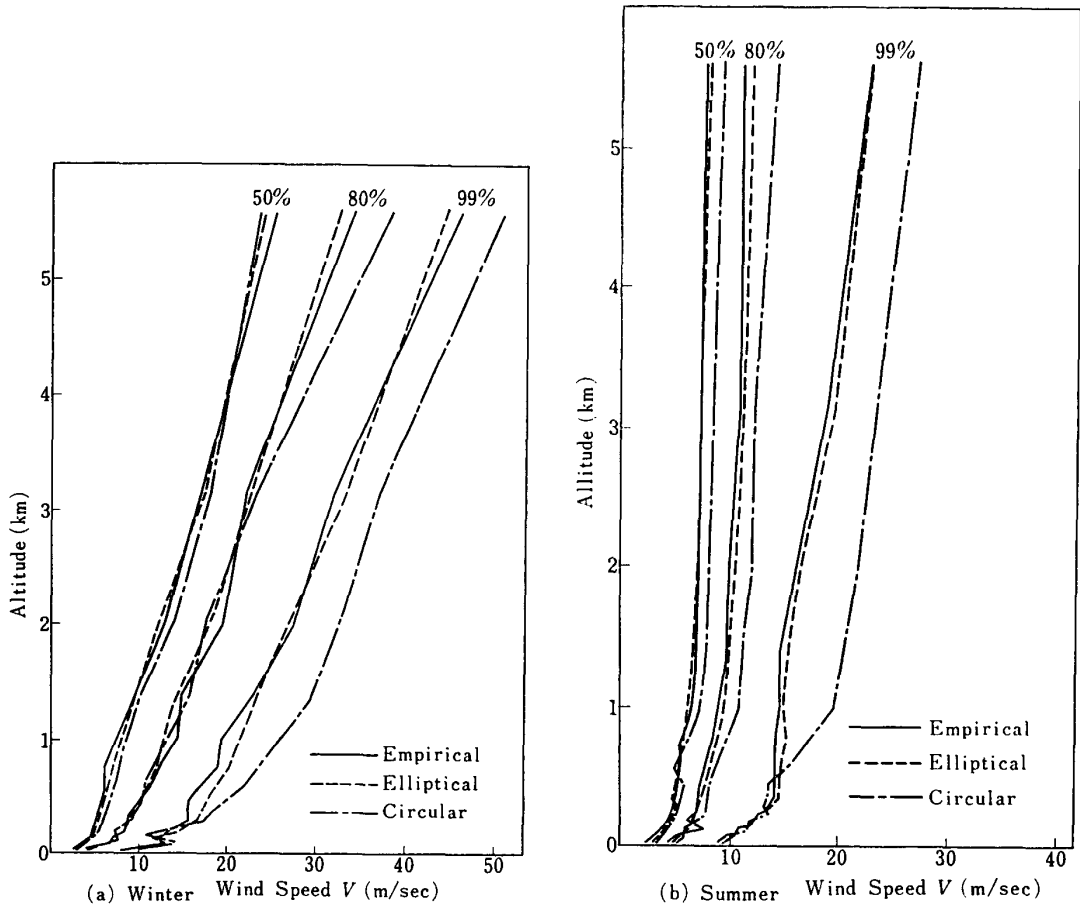


FIG. 6. Comparison of probability wind-speed profiles for KSC obtained by three methods.

basic data and because of the unknown amount of bias in the data, caution should be observed when considering the use of wind speed profiles. This limitation would be expected to apply generally to wind data obtained from the type of wind tracking radar used to gather the data considered herein. As shown in the previous section, relatively few parameters are required to define a generalized set of curves for wind-speed probability profiles when circularity is assumed. Such a set of curves is presented in Fig. 4.

If values of  $\bar{V}$  and  $\sigma$  are known, Fig. 4 can be used to determine either the probability of occurrence of a wind of magnitude  $V$  or the magnitude of wind  $V$  which will correspond to a particular probability.

The curves of Fig. 4 can also be used to determine wind-speed probability profiles at any location where  $\bar{V}$  and  $\sigma$  have been determined and where the assumption of a circular distribution is seemed valid.

### 3.4 Wind-Direction Probabilities

In a manner analogous to that used to obtain the wind-speed probabilities, wind-direction probability curves can be obtained; these curves include all wind speeds.

Presented in Fig. 7 is a limited set of comparison curves for KSC wind direction

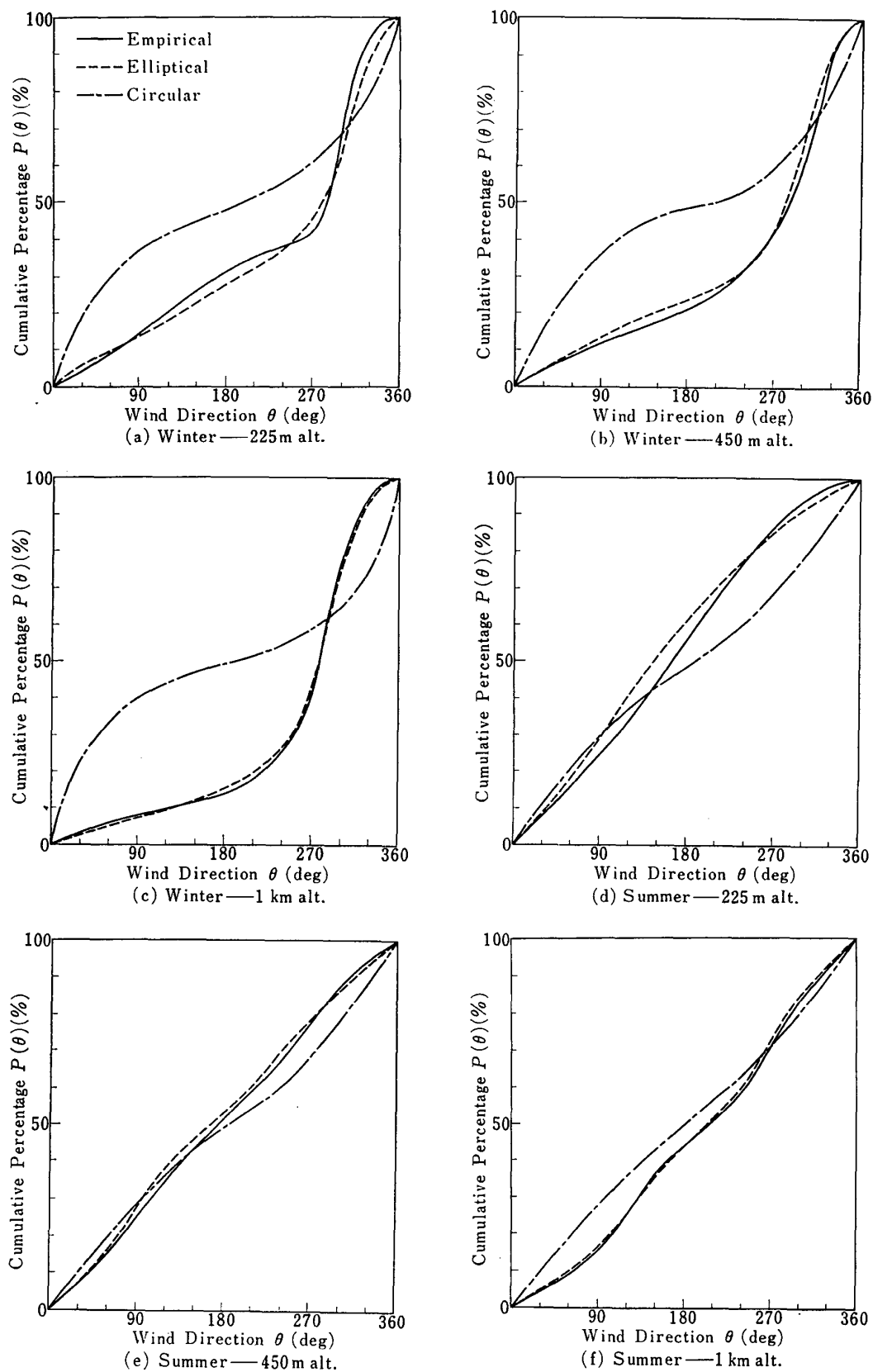


FIG. 7. Comparison of probability of wind-directions for KSC obtained by three methods.

probabilities as determined by the elliptical and circular binormal distribution methods and the empirical cumulative frequency methods.

On these curves  $P(\theta_i) = P(0 \leq \theta \leq \theta_i)$ . If  $P(\theta_1, \theta_2)$  is defined as the probability that  $\theta$  lies between  $\theta_1$  and  $\theta_2$  as  $\theta$  increases clockwise from  $\theta_1$  to  $\theta_2$ , the probability over any region can be found as follows:

$$\begin{aligned} P(\theta_1, \theta_2) &= P(\theta_2) - P(\theta_1) & (\theta_1 < \theta_2) \\ P(\theta_1, \theta_2) &= 1 + [P(\theta_2) - P(\theta_1)] & (\theta_1 > \theta_2). \end{aligned}$$

The main conclusion to be drawn from these curves is not the probability values but the fact that the elliptical method and empirical method of determining probability of direction are in excellent agreement in an altitude range above 450 meters at KSC. The circular distribution results are not in reasonable agreement with the results obtained by other two methods through the whole altitude range. Therefore, it seems reasonable to use elliptical distribution method for determining direction probabilities for KSC winds.

A set of generalized circular-wind-distribution probability of direction curves is presented in Fig. 5 for reference.

### 3.5 Component Wind Probability

The results presented in the previous subsections are wind directions considering all speeds. Although this type of probability information is often considered of prime interest, the problem of what wind speeds are within given probability limits in a given direction is also of considerable importance. This probability distribution is often referred to as the component wind probability envelope and is defined by the statistical marginal distribution along various sets of orthogonal axes—that is, the distribution includes all wind-speed components along these axes.

The problem of determining component winds is relatively simple even though the elliptical distribution method is used; in fact, it is about as simple as using the circular distribution method.

Typical elliptical component wind profiles for one, two and three sigma probabilities for KSC are presented in Fig. 8.

## 4. CONCLUDING REMARKS

Statistical parameters which define wind probabilities at KSC in an altitude range from 25 to 5600 meters have been determined.

Wind-speed probabilities, obtained by considering winds from all directions, and wind-direction probabilities, obtained by considering all wind speeds, were determined for KSC by three methods: the empirical cumulative frequency method and integration of the elliptical and circular binormal density functions over appropriate regions. It was concluded that the elliptical distribution method gave the best results for determining wind-speed and wind-direction probabilities for an altitude range above 450 meters; however, it was shown that the circular distribu-

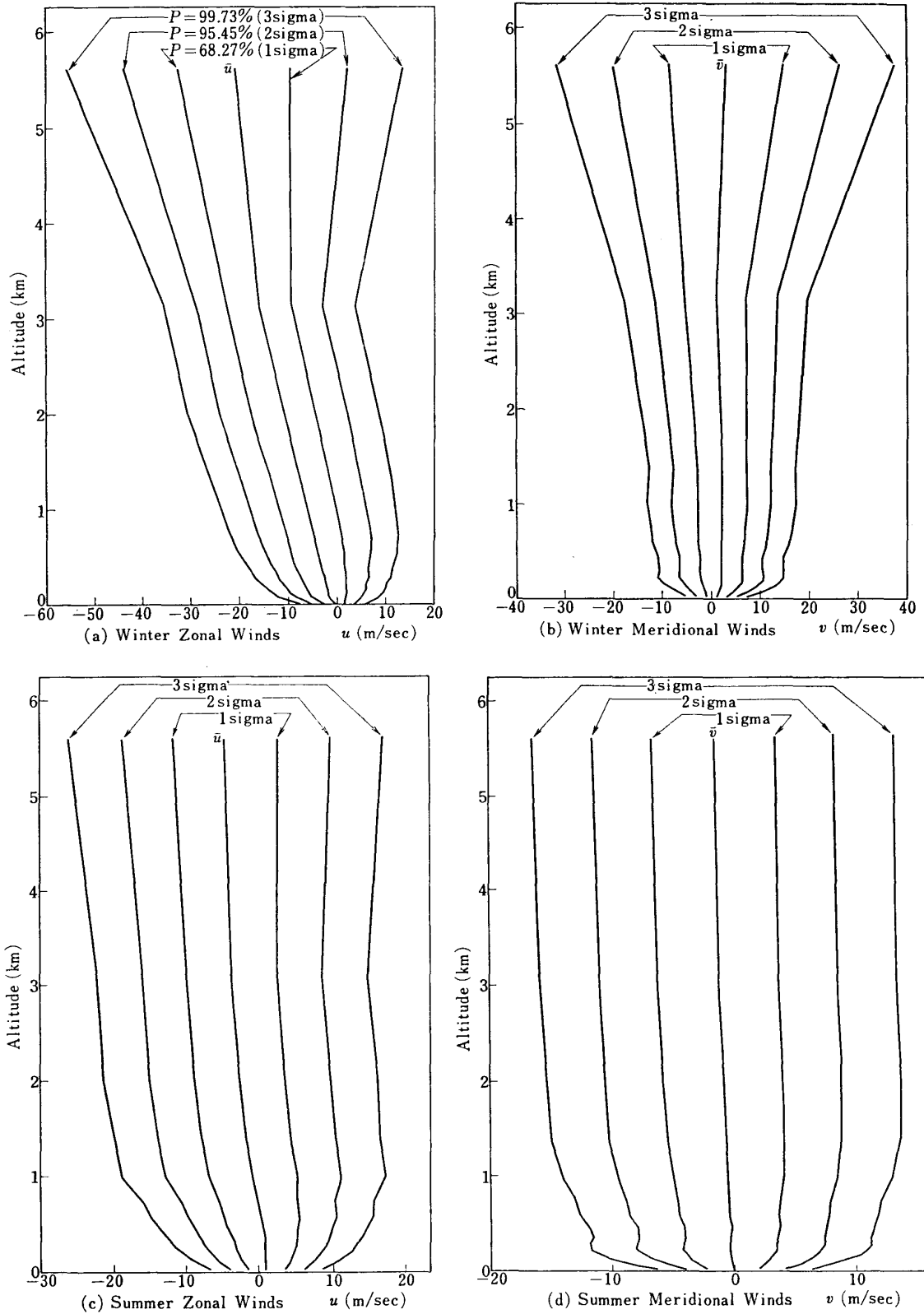


FIG. 8. Probability envelopes for component winds at KSC (Elliptical Distribution Method)

tion method did not give an adequate representation for these probabilities. General charts are presented for reference which can be used with tabulated values of statistical parameters to determine wind-speed and wind-direction probabilities by the circular distribution method; these charts can be used at any location for which the appropriate parameters are available and for which the assumption of circularity is valid.

#### ACKNOWLEDGEMENT

Acknowledgement is due to the members of balloon tracking group for wind observation at KSC for permission to utilize wind data in this paper. The author would like to express his sincere thanks to Mr. S. Nakao and Mrs. M. Mori for their helpful assistances in carrying out the computation and typing the manuscript.

*Department of Space Technology  
Institute of Space and Aeronautical Science  
University of Tokyo  
September 10, 1974*

#### REFERENCES

- [ 1 ] Reisig, G., "The Significance of Atmospheric Effects in Rocket Vehicle Technology", NASA TN D-1830, 1963.
- [ 2 ] Crutcher, H. L., "On the Standard Vector Deviation Wind Rose", *J. Meteor.*, 14, 1957.
- [ 3 ] Weaver, W. L., Swanson, A. G. and Spurling, J. F., "Statistical Wind Distribution Data for Use at NASA Wallops Station", NASA TN D-1249, 1962.
- [ 4 ] Tamaki, F., Nomura, T. and Matsuo, H., "Wind Compensation System in the Kagoshima Space Center, University of Tokyo", *Proc. 7th Inter. Symp. on Space Tech. and Science*, Tokyo, 1967.